frontiers | Frontiers in Physics

ORIGINAL RESEARCH
published: 10 May 2022
doi: 10.3389/fphy.2022.892037

An Eco-Friendly Phosphogypsum-Based Cementitious Material: Performance Optimization and Enhancing Mechanisms

Ziyan Wang[1], *Zhonghe Shui*[2,3], *Tao Sun*[2,3]* *and Zhiwei Li*[4]

[1]International School of Materials Science and Engineering, Wuhan University of Technology, Wuhan, China, [2]State Key Laboratory of Silicate Materials for Architectures, Wuhan University of Technology, Wuhan, China, [3]Advanced Engineering Technology Research Institute of Wuhan University of Technology, Zhongshan, China, [4]School of Materials Science and Engineering, Wuhan University of Technology, Wuhan, China

Little published data were effective in decreasing the setting time and improving the strength development of phosphogypsum-based supersulfate cement (P-SSC) containing an excess of 40% phosphogypsum to achieve adequate field working and mechanical properties. This study aimed to optimize the application performance of P-SSC by wet grinding, the enhancement mechanism of which was discussed further. The wet grinding mainly refined and dispersed the phosphogypsum with the large particle size, improving the formation of ettringite by increasing the supersaturation of phosphogypsum. However, the release of impurities prolonged the setting time of P-SSC pastes, leading to a lower early strength. Short-time wet grinding destroyed the surface structure of slag with the small particle size, presenting a higher hydration degree. It seemed to have a more significant improvement of generated C-(A)-S-H gel, while treating P-SSC by wet grinding slightly enhanced strength development. Increasing the aluminate concentration by incorporating active aluminum phases in this process significantly promoted the generation rate of ettringite and weakened the negative effect of impurity release. Therefore, a feasible and effective method to prepare P-SSC pastes was proposed to realize the large-scale application of phosphogypsum in the building materials industry.

Keywords: phosphogypsum-based supersulfate cement, wet grinding, aluminum phases, hydration phase assemblage, application performance

OPEN ACCESS

Edited by:
Wenxiang Xu,
Hohai University, China

Reviewed by:
Shiyu Sui,
Qingdao University of Technology, China
Fengjuan Wang,
Southeast University, China
Guo Wen Sun,
Shijiazhuang Tiedao University, China

***Correspondence:**
Tao Sun
sunt@whut.edu.cn

Specialty section:
This article was submitted to Soft Matter Physics, a section of the journal Frontiers in Physics

Received: *08 March 2022*
Accepted: *28 March 2022*
Published: *10 May 2022*

Citation:
Wang Z, Shui Z, Sun T and Li Z (2022) An Eco-Friendly Phosphogypsum-Based Cementitious Material: Performance Optimization and Enhancing Mechanisms. Front. Phys. 10:892037. doi: 10.3389/fphy.2022.892037

INTRODUCTION

Phosphogypsum, solid waste from phosphoric acid production, is released at a rate of 170 million tons per year and is expected to accumulate over 7 billion tons by 2025 worldwide [1]. In the absence of effective treatment for phosphogypsum with poor properties compared to natural gypsum, small amounts of phosphogypsum are used as retarders or to make gypsum board, where the utilization ratio is lower than 40%. Effective recycling mechanisms need to be given to lower the accumulation of phosphogypsum, as required by the Law of the People's Republic of China on the prevention and management of environmental contamination by solid waste. According to the hydration mechanism of supersulfate cement (SSC), Lin et. al [2, 3] have prepared phosphogypsum-based supersulfate cement (P-SSC), containing more than 40% phosphogypsum, 40%–50% slag, and a small amount of alkali activator. Previous studies have demonstrated that the P-SSC presents

excellent water resistance and volume stability, as well as corrosion resistance of chloride ions, which is better than Portland cement and slag cement [4, 5]. As an eco-friendly cementitious material presented comparable mechanical properties with original Portland cement, P-SSC is projected to be used as an alternative in practical engineering. However, the soluble and eutectic fluorine and phosphorus show a negative effect on the hydration and concretion of P-SSC, leading to a more extended setting and lower strength [6]. At present, increasing workability and mechanical performance of P-SSC has become a crucial problem for realizing the application.

Ettringite, as the main hydration product of gypsum–slag cementitious material, also shows a significant promotion for concretion and strength development [7, 8]. The previous studies on the formation rate and stable existence of ettringite pay more attention to the ion concentration, pH, and temperature in the pore solution. Shi et al. pointed out that the Ca^{2+} concentration in solution was the key factor affecting the generation rate and stability of ettringite by comparing the ettringite production of cement with different C_3S and C_2S contents at the initial hydration stage [9]. Wang revised this view that the expansion characteristics of ettringite depend on the concentration of OH^-, which as a part of crystal structure promotes the nucleation and growth of ettringite [10]. Lou et al. believed that the generated rate of $[Al(OH)_6]^{3-}$octahedron was the lowest in the establishment process for ettringite structure as the dissolution and release rate of AlO_2^- from C_3A is slower than that of gypsum [11, 12]. Compared with C_3A, CA presents a higher hydration rate and equilibrium concentration of AlO_2^- in pore solution, leading to the rapid crystallization of ettringite. The generated ettringite requires the participation of OH^-, while the change of pH in pore solution will affect the morphology and stability of ettringite, for which the stable environmental pH ranges from 10.5 to 13 [13]. Gypsum will dissolve and generate portlandite in the environment containing a high concentration of NaOH, thus promoting the formation of other phases rather than ettringite. Therefore, the effective methods to accelerate the generation rate of non-expansibility ettringite by increasing the ion release rate and keeping it existing steadily need to be considered for helping shorten the setting time and optimizing the microstructure of P-SSC.

Particle refinement is regarded as an effective method for increasing the dissolution and hydration rate of cementitious materials [14, 15]. The rapid generation of gelatinous structure and enhancement of the hydration degree can compensate for the negative effects of impurities to meet the performance requirement of P-SSC binders in actual application [6, 16]. Compared with dry grinding, published data have reported that grinding in a water environment (i.e., wet grinding) can effectively reduce the energy consumption caused by excessive surface energy, presenting a higher efficiency [17–19]. Therefore, wet grinding is considered for preparing P-SSC pastes in this study. The effect mechanism on the hydration process of different particles is investigated further, where the particle size distribution and Zeta potential are used to characterize the refining and dispersion of wet grinding on phosphogypsum and slag, respectively. In addition, the promotion of the active aluminum phase introduced by metakaolin on ettringite formation is also explored in this process based on the previous studies. Combined with the hydration assemblage evolution, setting time and mechanical properties are measured to evaluate the application performance. A feasible preparation and control methods are proposed to realize efficient reuse of phosphogypsum.

EXPERIMENTAL PROGRAM

Raw Materials

As shown in**Table 1** and **Figure 1**, phosphogypsum and P. II. 42.5 cement, with the same ratio in all P-SSC samples, were provided by Hubei Yihua Limited liability company and Huaxin Cement Limited liability company, respectively. As the primary supplement materials, slag with a middle particle size (D_{50}) of 10.9 μm was supported by Wuhan Iron and Steel Limited liability company. Compared with slag, metakaolin with great volcanic activity presented higher Al_2O_3 content and smaller particle size (D_{50} = 4.4 μm). Metakaolin was produced by Maoming Kaolin Technology Limited liability company. Phosphogypsum and P. II. 42.5 cement displayed relatively large particles, in which D_{50} reached 33.9 and 11.60 μm, respectively.

Mix Proportions and Sample Preparation

The mix proportions and preparation methods of all samples are listed in **Table 2** and **Figure 2** to explore the primary effect of wet grinding on strength development. It is worth noting that the aim of pretreatment for fresh phosphogypsum was weakening the retardation and negative effect on strength development caused by impurity precipitation, such as soluble phosphorus and fluorine. After wet grinding and aging, the pH value of phosphogypsum incorporated a small amount of alkali activator increased gradually and existed 10.8, leading to the soluble phosphorus existed as PO_4^{3-} in pore solution and was precipitated as insoluble calcium phosphate. The addition of the modifier was needed to keep the pH value of modified phosphogypsum exceeded 11.8, which is most suitable for the generation of ettringite. Previous research has reported that the pH value of modified phosphogypsum showed a positive correlation with the content of steel slag regarded as a modifier. When the content of steel slag reached 3–4%, the pH value exceeded 12, after which the improvement rate displayed a decreasing trend [2]. Therefore, the mass ratio of 4% for P. II. 42.5 cement was chosen to adjust the pH value of modified phosphogypsum to reach around 12 and incorporated a bit of slag as the calcium source for the precipitation of impurities. In addition, the aging time needed to exceed 8 h to confirm the precipitation adequately. The whole pretreat process was described as wet grinding fresh phosphogypsum for 30 min with slag and P. II. 42.5 cement (i.e., phosphogypsum:slag:P. II. 42.5 cement = 94:2:4 and water/solid (w/s) = 0.6), then aging for 24 h, where the mass ratio of zirconia balls (6 cm:5 cm:3 cm: 2 cm = 1:3:6:2) to powder was 6:1.

All samples with the same water/binder (w/b) of 0.5 contained 45% modified phosphogypsum and 5% P. II. 42.5 cement, where

TABLE 1 | Chemical composition of main oxides (wt%) of raw materials by XRF.

Oxide	Al_2O_3	SiO_2	Fe_2O_3	Cao	K_2O	TiO_2	SO_3	P_2O_5	Na_2O	MgO	F	LOI
Phosphogypsum	1.09	7.5	0.44	27.05	0.6	0.12	37.75	0.948	0.17	0.06	1.83	20.77
P. II. 42.5 cement	6.45	21.75	3.24	58.02	0.74	0.51	2.47	0.25	0.14	2.25	–	3.8
Slag	15.16	32.95	0.21	40.14	0.4	0.71	2.27	0.01	0.27	7.29	–	0.58
Metakaolin	38.72	56.71	0.77	0.06	0.56	0.28	0.13	0.45	0.38	0.11	–	1.79

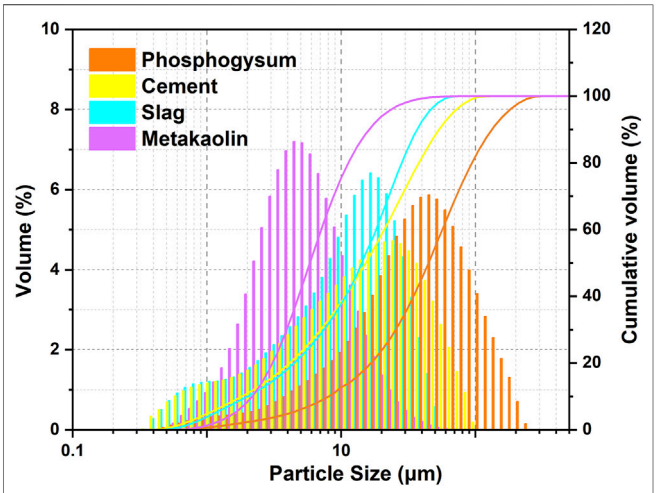

FIGURE 1 | Particle size distribution of raw materials.

W1 and W4 were mixed and wet-grinded, respectively. In comparison, W2 and W3 were prepared by wet grinding phosphogypsum and slag, respectively, for 30 min, then mixing all raw materials as the proportion designs. Significantly, the influence of the active aluminum phase on solidification and mechanical properties was also investigated by designing sample WK10, which incorporated 10% metakaolin and was prepared by wet grinding for 30 min. The wet grinding and mixing process relied on a ceramic ball mill and a power-driven revolving pan mixer. All P-SSC pastes were molded as cubic with a side length of 40 mm for the microstructure tests. Referring to GB/T 17671-1999 [26], the samples for mechanical properties tests were prepared by mixing cementitious materials and standard sand with a mass ratio of 1:3 and molded as rectangular specimen mortars with a size of 40 mm × 40 mm × 160 mm. All specimens were kept in the standard condition of 20 ± 2°C with a relative humidity of 96 ± 2% until the testing age.

Testing Methods

Particle Size Distribution

The particle size distribution of all raw materials and fresh pastes was characterized by Malvern Mastersizer 2000 to evaluate the main effect of wet grinding on different particles. Alcohol as a dispersant was carried out for dispersing particles of pastes in this test, where the measured range was located in 0.02–2,000 μm.

Zeta Potential

Zeta potential as a characteristic reflected the dispersion performance of particles in the fresh slurry, in which the absolute value was associated with the stability of colloidal particles [20]. The paste needed to be diluted into a suspension to recognize colloidal particles and filled into an electrophoresis chamber for the test when the particles tended to be stable. The average value was regarded as the Zeta potential by measuring the electric displacement of nine particles.

Setting Time

As an essential index for workability, setting time was affected by the comprehensive effect of impurity precipitation and hydration rate. According to GB/T 1346-2011 [21], the depth of the Vicat needle inserted in the P-SSC pastes with normal consistency was measured to determine the time to reach the initial and final settings.

pH Value

The pore solution of all P-SSC samples after hydration for 1 h was tested to verify the effect of impurity release on the increased rate of alkalinity. The fresh slurry was centrifuged at high speed to obtain the supernatant, which is regarded as the pore solution, whose pH values were evaluated by a Leici pH meter.

TABLE 2 | Mix proportions of specimens (wt%).

Sample label	Modified phosphogypsum (wt%)	Cement (wt%)	Slag (wt%)	Metakaolin (wt%)	Water/ binder (w/b)	Treatment method
W1	45	5	50	0	0.5	Mixing all raw materials directly for 4 min
W2	45	5	50	0	0.5	Wet grinding modified phosphogypsum for 30 min and mixing with other raw materials for 4 min
W3	45	5	50	0	0.5	Wet grinding slag for 30 min with W/S = 0.5 and mixing with other raw materials for 4 min
W4	45	5	50	0	0.5	Wet grinding all raw materials for 30 min
WK10	45	5	40	10	0.5	Wet grinding all raw materials for 30 min

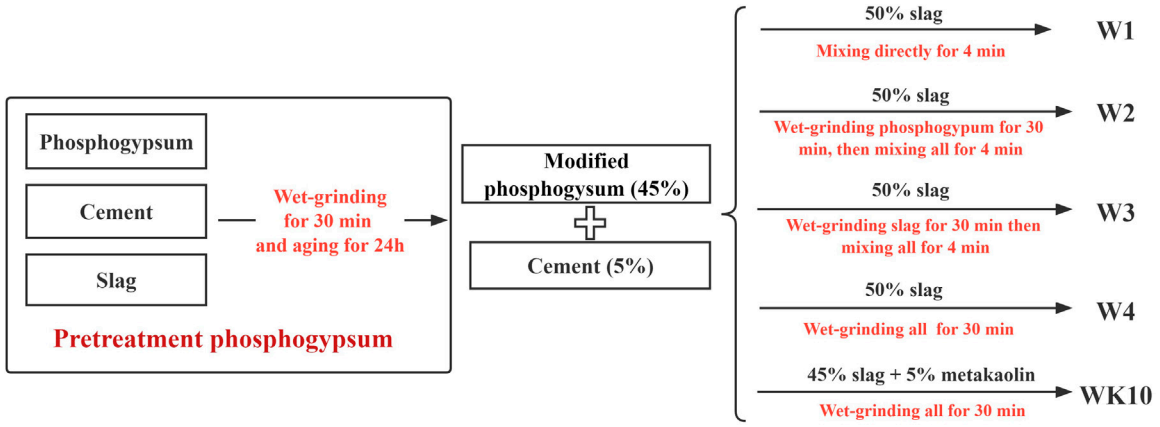

FIGURE 2 | P-SSC paste preparation process in this study.

X-Ray Diffraction

The P-SSC binders cured for 28 d were selected to characterize the hydration assemblage evolution, determining the enhancement mechanism of wet grinding and incorporating active aluminum phases. All samples were crushed into powder and sieved through a fine screen with a pore size of 63 μm. Then, the powder was kept in anhydrous ethanol for solution change and dried in vacuum at 40°C. XRD, FTIR, ^{27}Al NMR, and TG-DSC tests were carried out on the obtained samples.

The crystalline phases of P-SSC binders were characterized by XRD (Bruker D8 Advance) equipped with CuKα X-ray in the test condition of 40 kV and 40 mA. The measuring scope of all XRD spectra was in the range of 5°–90° 2θ. The relative mass (W) among the different minerals can be evaluated by X-ray diffraction (XRD)/reference intensity ratio (RIR) analysis when the composition of hydration products was relatively simple. According to **Eqs 1**, **2**, the integral intensity I of the prominent peak for the mineral phase can be calculated by Jade 6, and the subscript i represents the type of mineral. RIR denoted the reference intensity ratio of mineral phase obtained from the PDF card of the International Centre for Diffraction (ICDD) or measured by experiment. With this method, we can approximate the relative content of the ettringite and unreacted gypsum to determine the hydration degree of this system [22, 23].

$$W_i = \frac{I_i/RIR_i}{\sum_{i=1}^{n}(I_i/RIR_i)} \quad (1)$$

$$\sum_{i=1}^{n} W_i = 1 \quad (2)$$

Fourier Transform Infrared Spectroscopy

The characteristic bands located in the mid-infrared region of 400–4,000 cm^{-1} can be reflected by FTIR, which was regarded as supplementary method to describe the change in amorphous phases, such as the polymerization of C-(A)-S-H gel and the existence of AH_3 gel. The slices prepared by the mixed powder of P-SSC and KBr with a ratio of 1:100 were measured by using a Nexus spectrometer.

^{27}Al Nuclear Magnetic Resonance

The aluminum phases that existed in raw materials and hydration products were characterized by ^{27}Al NMR, which was considered an indicator to evaluate the hydration degree of supplement cementitious materials and the relative content of hydration products. P-SSC powder was packed into rotors with a diameter of 4 mm and compacted for the test, where the ^{27}Al NMR experiment was conducted with a pulse width of 1 μs and a recycle delay of 2s with 1,024 scans. In addition, the $AlCl_3$ solution was regarded as a reference, and the deconvolution of ^{27}Al NMR spectra was analyzed by PeakFit software, where the Lorentzian/Gaussian function was consistent with 0.8.

X-Ray Photoelectron Spectroscopy

ESCALAB 250Xi photoelectron spectroscopy (Thermo Fisher, United States) equipped with a monochromatic Al Ka source was carried out to test the electron binding energies of the main elements in the samples, aiming to determine their forms in the hydrated phases. The background pressure of the analysis chamber was set at about 4×10^{-8} mbar, and the monitoring values were about 14.2 kV and 11.3 mA. A charge compensation standard was adopted for the samples, where the C 1s peak (284.8 eV) was used to calibrate all spectra [24].

Thermal Gravimetric–Differential Scanning Calorimetry

The mass loss of free and structural water existing in different substances can be measured by TG-DSC to evaluate the relative content of hydration products within the same weightlessness intervals. An SDT Q 600 calorimeter was employed on P-SSC binders in the range of 25–800°C with 10°C/min under an air atmosphere.

Strength Development

The compressive and flexural strength of all P-SSC pastes at 3 days, 7 days, and 28 days was tested as per GB/T 17671-1999 [25]. Three water-saturated mortars with dry surfaces were measured by using a 3,000 kN compression machine and loaded at a rate of 2.4 kN·s at test ages. The average value was reported and standard deviation was obtained.

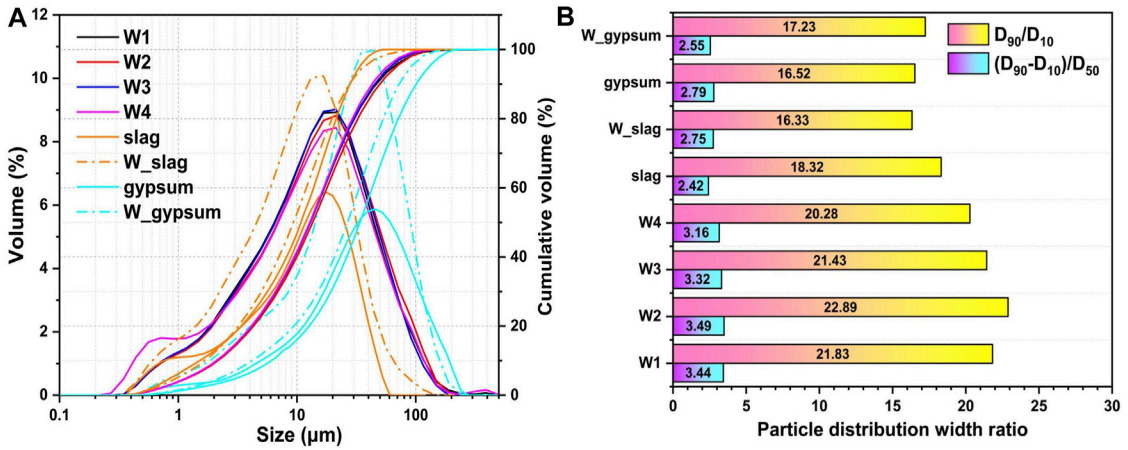

FIGURE 3 | (A) Particle size distribution and **(B)** width ratio of P-SSC pastes, slag, and phosphogypsum before and after wet grinding.

TABLE 3 | Characteristic particle size parameter of P-SSC pastes.

Sample label	D_{10}	D_{50}	D_{90}
W1	2.70	16.35	58.94
W2	2.75	17.25	62.96
W3	2.68	16.49	57.43
W4	2.68	16.34	54.34
slag	1.52	10.87	27.85
W_slag	2.14	11.92	34.94
gypsum	6.09	33.88	100.58
W_gypsum	5.34	33.98	92.01

RESULTS AND DISCUSSION

Particle Size Distribution and Zeta Potential

With the purpose of investigating the effect of wet grinding on particle fining and particle bulk density for the fresh P-SSC slurry, the particle size distribution and characteristic parameters of four fresh pastes, slag, and phosphogypsum before and after wet grinding are described in **Figure 3**. Three characteristic parameters of particles listed in **Table 3**, that is, D_{10}, D_{50}, and D_{90}, are carried out to determine the content change in particles of different sizes [26, 27]. In addition, the particle distribution width ratios of χ_1 and χ_2 have been used for discussing the effect of wet grinding on the concentrated and uniform samples effectively, where χ_1 and χ_2 are described by **Eqs 3**, **4**; [15, 17]. A more uniform particle is observed when the calculated value is smaller.

$$\chi_1 = \frac{(D_{90} - D_{10})}{D_{50}} \tag{3}$$

$$\chi_2 = \frac{D_{90}}{D_{10}} \tag{4}$$

Compared with modified phosphogypsum, the particle size distribution curve for W_gypsum shifts to the left and three characteristic parameters reduce significantly, where D_{90} decreases from 100.58 to 92.01 μm. It implies that wet grinding plays a practical fining effect on the large particle of phosphogypsum, rather than the slag with a small particle size as the energy efficiency of wet grinding decreases and eventually approaches 0 with the further refinement of particles [28]. On the contrary, the characteristic particle size parameters of slag show a slight increase after wet grinding, which may be associated with the agglomeration phenomenon caused by the change of surface charge.

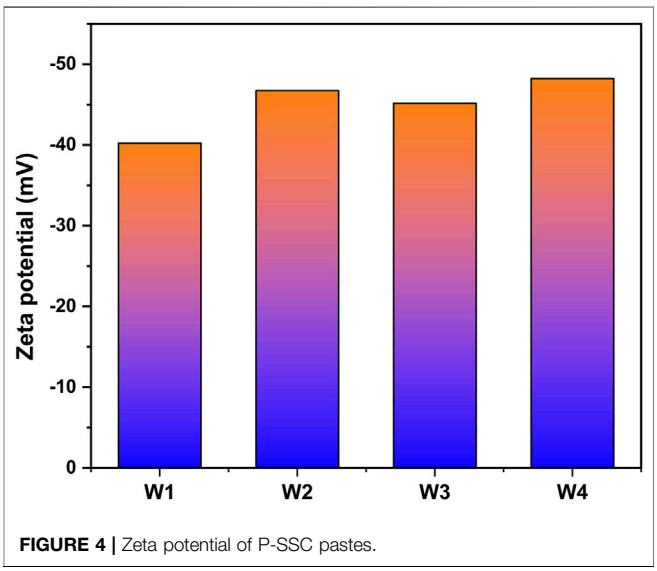

FIGURE 4 | Zeta potential of P-SSC pastes.

For fresh P-SSC slurries, the characteristic particle size parameters show little difference, where D_{10}, D_{50}, and D_{90} locate in the range of 2.65–2.75 μm, 16.30–17.30 μm, and 54.00–63.00 μm, respectively. Compared to W1, the particle size parameters reach the smallest in W4 while displaying an increased trend in W2. As **Figure 3B** described that χ_1 and χ_2 of W3 and W4 show a reduction, implying that the wet grinding makes the particle distribution width of P-SSC narrowed and improves the uniformity. However, the decreasing trend is

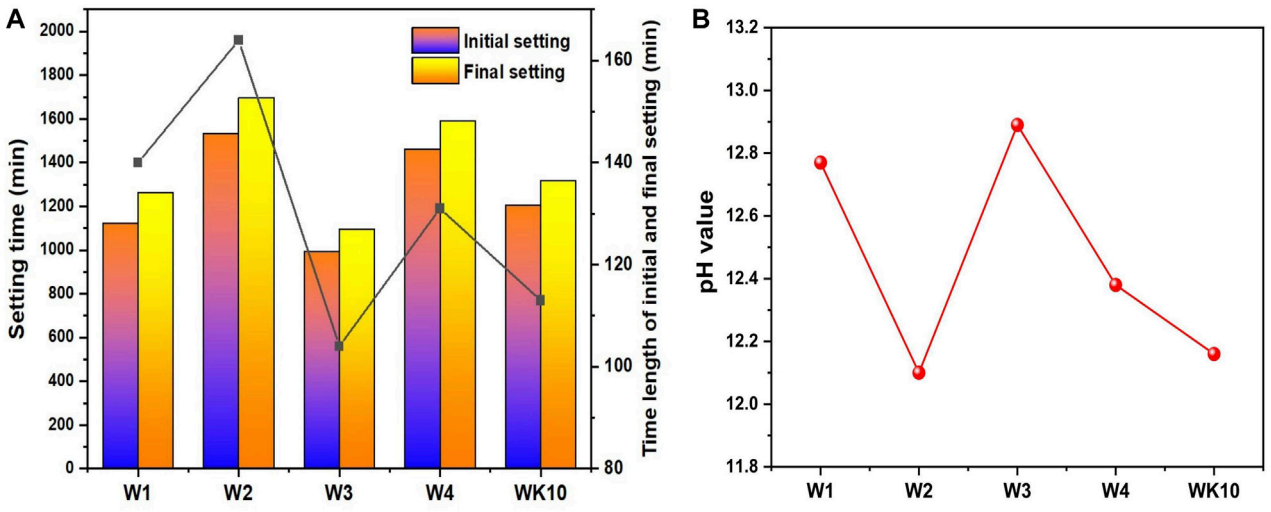

FIGURE 5 | (A) Initial and final setting times and **(B)** pH value of P-SSC pastes.

noticed in the particle size and χ_1 of phosphogypsum after wet grinding, which is the opposite of slag. It also proved that wet grinding has an efficient refining effect on phosphogypsum with large particle size, presenting a more remarkable decrease of D_{10} than D_{90}. On the contrary, the increase in D_{10} and D_{90}, as the agglomeration and hydration of slag after wet grinding, results in an enhancement in χ_1. Therefore, materials with different hardness or in various working conditions will present the distinguishing refining effect after wet grinding.

The Zeta potentials of P-SSC slurry characterize the relationship between particle size distribution and stability. As **Figure 4** displays, the process of short-time wet grinding improves the stability and dispersion of fresh slurry. With the acceleration of hydration rate, the generation of flocculation structure and change of surface charge may lead to particle agglomeration, manifesting the increase in particle size. In addition, W2 shows higher absolute Zeta potential than W3, indicating that wet grinding has a significant effect on the refinement and dispersion of phosphogypsum, and W2 presents the most excellent stability [29, 30]. However, the wet grinding process shows a limited effect on refining slag particles, which slightly promotes strength development.

Setting Time and pH Value

The setting time of all P-SSC pastes is described in **Figure 5A** to ensure that the dominant factor affects the early hydration rate. All pastes present much longer setting times than Portland cement, where the initial and final settings reach 16–26 h and 18–28 h, respectively. Referring to W1 with initial and final setting times of 1122 min and 1262 min, respectively, a shorter setting time is observed in W3, of which the initial and final settings reduced around 11.10% and 13.87% severally. It means that wet-grinding slag accelerates the hydration rate and promotes the increase in pH in the pore solution (**Figure 5B**). On the contrary, wet-grinding phosphogypsum further results in a more significant retarding effect in the P-SSC samples, where the time length between the initial and final settings increases, which is consistent with the results of the pH values. In comparison with W1, an inhibition effect on the pH value is verified in W2, W4, and WK10 after hydration for 1 h, in which the phosphogypsum gets wet grinded again. The refining of wet grinding will promote the dissolution and supersaturation of phosphogypsum, as well as the release of impurities. More portlandite is consumed for impurity precipitation, which will delay the increased rate of pH for pore solution, leading to a lower hydration rate. Compared with W4, incorporated 10% metakaolin has a positive effect on setting time, implying that the rapid hydration of the active aluminum phase can mitigate the impact of impurity release on coagulation for P-SSC.

Hydration-Phase Assemblage

The results of XRD (**Figure 6**) prove that the hydration products in P-SSC binders prepared by wet grinding present no difference from the reference W1, where ettringite and gypsum as the main hydration phases are noticed. In contrast, other phases such as portlandite with a prominent diffraction peak at 28.9° 2θ and C-S-H gel with diffuse peaks are slight. It implies that the absence of portlandite may limit the continuous hydration process during the later hydration period. According to **Eq. 1**, the relative ratio of ettringite and unreacted gypsum is characterized based on the RIR method to evaluate the influence of wet grinding and incorporated aluminum phase on the generation of ettringite. The samples prepared by wet grinding contain more ettringite than W1 prepared by mixing directly, indicating that the process of wet grinding accelerates the dissolution of phosphogypsum and slag. Especially, wet grinding for modified phosphogypsum and slag, respectively, seems to show notable improvement in the formation of ettringite, where the relative ratio of ettringite in W2 reaches 28.62%. In addition, the active aluminum phase as the main factor demonstrates the hydration rate of ettringite at the initial period. Compared to W4, the sample containing 10% metakaolin displays a higher content of ettringite, implying

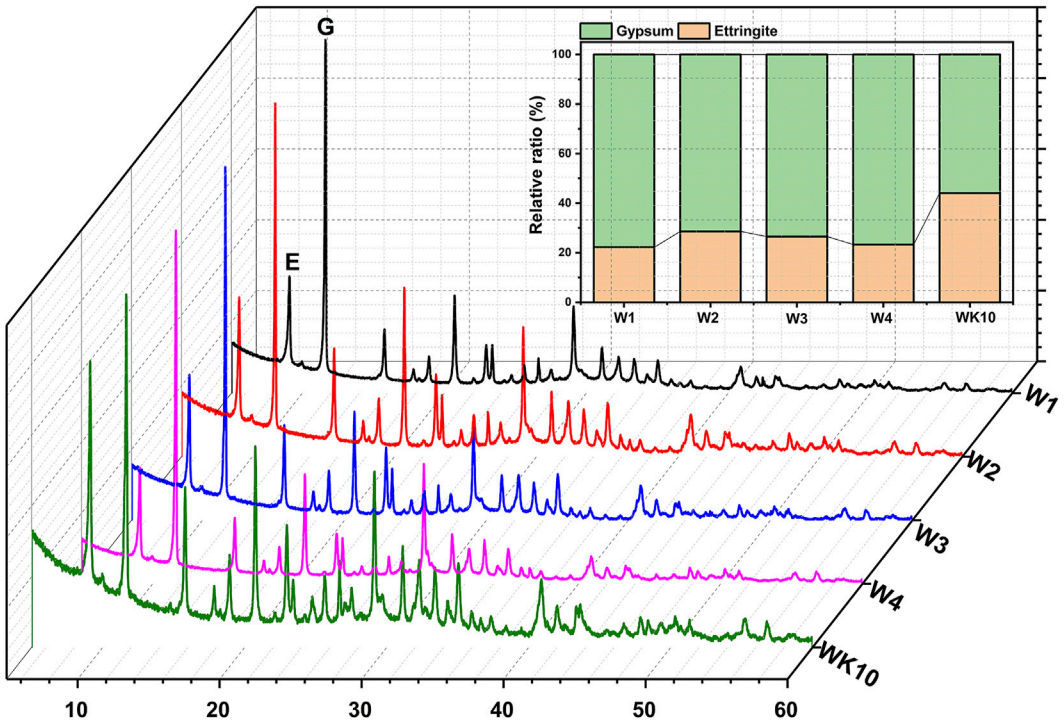

FIGURE 6 | XRD patterns of P-SSC binders at 28 days.

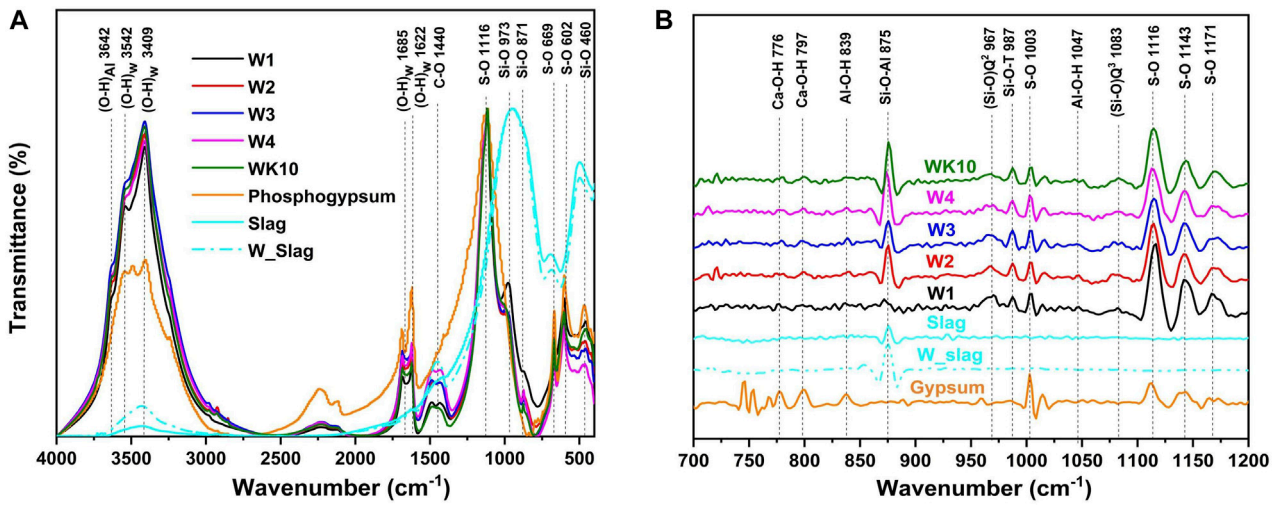

FIGURE 7 | FTIR spectra of P-SSC binders at 28 days, slag, and phosphogypsum; **(A)** transmittance (T) *vs*. wavelength (W); **(B)** 2nd derivative of the transmittance d^2T/dW^2 *vs*. wavelength.

that the rapid dissolution of metakaolin during wet grinding has effectively increased the concentration of AlO_2^- in the pore solution and accelerated the hydration rate in the gypsum-saturated solution.

FTIR spectra of all samples are described in **Figure 7A**. The wet grinding treatment increases the structural water content of slag, presenting an enhancement of the asymmetric and symmetric stretching vibration of O-H, whose characteristic band is located at around 3,428 cm^{-1}. In addition, the band at 490 cm^{-1}, which is associated with Si-O bending vibration in slag, presents a reduction after wet grinding as the surface structure of slag is destroyed. Therefore, a few portlandite, [≡Si-O-] and [≡Al-

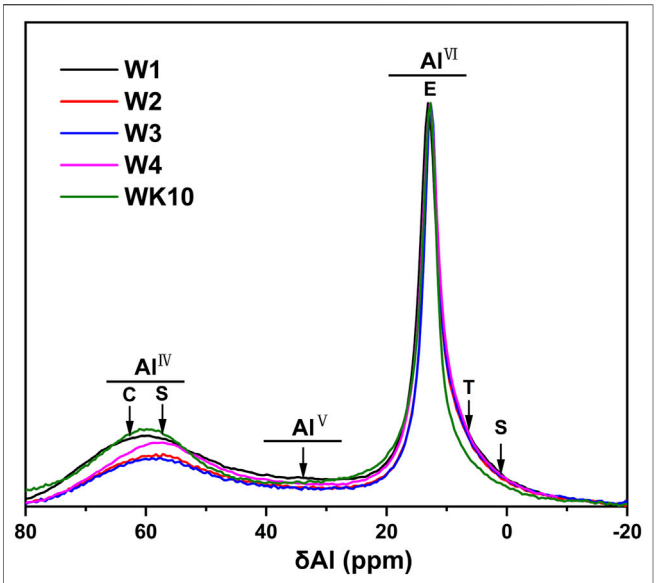

FIGURE 8 | ^{27}Al NMR spectra of P-SSC binders at 28 days.

O-] are released into the pore solution [31]. Combined with the 2nd derivative results of transmittance (**Figure 7B**), an increase in bands located in the range of 800–900 cm^{-1} also certifies that wet grinding has a positive effect on strength development by improving the hydration activities of slag. A published study has proved that the band of S-O vibration at 1,004 cm^{-1} in unhydrated gypsum and ettringite can be deconvoluted into four peaks at 1,116 cm^{-1}, 1,143 cm^{-1}, 1,171 cm^{-1}, and 1,098 cm^{-1}, which may correspond to the degenerate and non-degenerate modes of SO_4^{2-} units occupying different positions [32]. Therefore, the bands situated within 1,100–1,200 cm^{-1} are recognized as the vibration of S-O.

The generation of hydration products such as C-(A)-S-H gel and ettringite will promote the free water transformation into structural water, enhancing characteristic bands in the scope of 4,000–2,900 cm^{-1}. As **Figure 7A** shows, wet grinding improves the hydration degree of P-SSC binders, where the O-H stretching vibration in WK10 and W3 is stronger than that in W1, while opposite trends are noticed for the bands located in a range of 400–800 cm^{-1}, which is associated with unhydrated slag, meaning a lower hydration degree in the sample without wet grinding. For W1, the characteristic bands of Q^2(Si-O) stretching vibration within 950–1,000 cm^{-1} present the most prominent strength and amplitude due to the large content of C-S-H gel with short chain [33, 34]. On the contrary, a significant band of Q^3(Si-O) stretching vibration at 1,003 cm^{-1} is observed in other samples, especially in W4 and WK10, which is associated with the increase in polymerization for C-(A)-S-H gel. In addition, an enhancement of bands for Al-O-H bending and symmetric vibration (i.e., the bands centered at 839 cm^{-1} and 1,047 cm^{-1} in **Figure 7B**) indicates that wet grinding promotes the generation of hydration product contained aluminum phases, such as AH_3 gel and ettringite [35, 36].

Strength development and microstructure optimization of P-SSC binders are related to the hydration degree. Based on the analysis of XRD and FTIR, ^{27}Al NMR is carried out to characterize the content of AlO in the different chemical environments. The relative ratio of unreacted and reacted AlO is measured further to evaluate the effect of wet grinding and extra aluminum phase on the hydration process, providing an optimum proposal of application performance for P-SSC based on the microstructure evolution. The test results of ^{27}Al NMR are normalized, as described in **Figure 8**; two significant peaks located in the range of 0–20 ppm and 40–70 ppm are observed in all samples, where the AlO existed in C-A-S-H gel, ettringite, and AH_3 gel can be distinguished by the signals at 65 ppm, 13 ppm, and 9.5 ppm. In addition, the unreacted AlO in slag and metakaolin exists in the form of Al^{IV}, Al^{V}, and Al^{VI}, which locates at 57 ppm, 33 ppm, and 1.9 ppm severally. For the P-SSC samples with the same mix proportion (i.e., W1, W2, W3, and W4), the relative intensity of the peak in the scope of 0–20 ppm reaches the highest in W2, associated with the high content of ettringite. On the contrary, W1 and WK10 display a high content of unreacted AlO, appearing at a stronger peak within 40–70 ppm [37]. In addition, the ^{27}Al NMR curves are deconvoluted into six peaks to determine the relative and absolute content of AlO in the different environments (**Figure 9**). Wet-grinding phosphogypsum and slag, respectively, improve the formation of ettringite significantly, while incorporating metakaolin increases the content of Al^{IV} due to the high reserve of aluminum and silicon phases [38]. In contrast to W2, W3 displays a larger area for the peak depending on generated C-A-S-H gel, meaning that the rapid hydration of slag trends to form gels rather than ettringite.

As **Figure 10A** shown, the sample prepared by mixing directly presents a high content of Al^{IV} and Al^{V} in unreacted slag, and the variation tendency of the ettringite content is consistent with XRD analysis, where the relative AlO content in ettringite for W2 reaches 40.97%. It demonstrates that wet grinding has notable refining and dispersion effect on phosphogypsum with large particles. The increase of dissolution and supersaturation in phosphogypsum promotes the generation of ettringite, resulting in a higher hydration degree of P-SSC binders. Similarly, the destruction of the surface structure for slag by wet grinding also accelerates the release of the aluminosilicate group, presenting reacted AlO in binders reaches 70%, while W1 still contained 39% unreacted AlO (**Figure 11**). According to the XRF results for raw materials, the absolute AlO in each substance is calculated further and described in **Figure 10B**. Combined with the deconvolution results, more aluminum silicates or aluminum gels are observed in W3 and W4, presenting a stronger peak centered around 9.5 ppm, which is regarded as AH_3 gel in this study due to the low content of portlandite in pore solution. However, the sample prepared by wet grinding all raw materials (i.e., W4) displays a low hydration degree, which may be affected by the impurities that existed in phosphogypsum and the location of generated hydration products. The wet grinding process destroys the lattice structure, leading to an arresting retard effect of P-SSC pastes by releasing more phosphate groups into pore solution and slowing the development rate of the pH value. For slag with a high hydration rate, more aluminate groups will react with dissolved gypsum or portlandite to generate

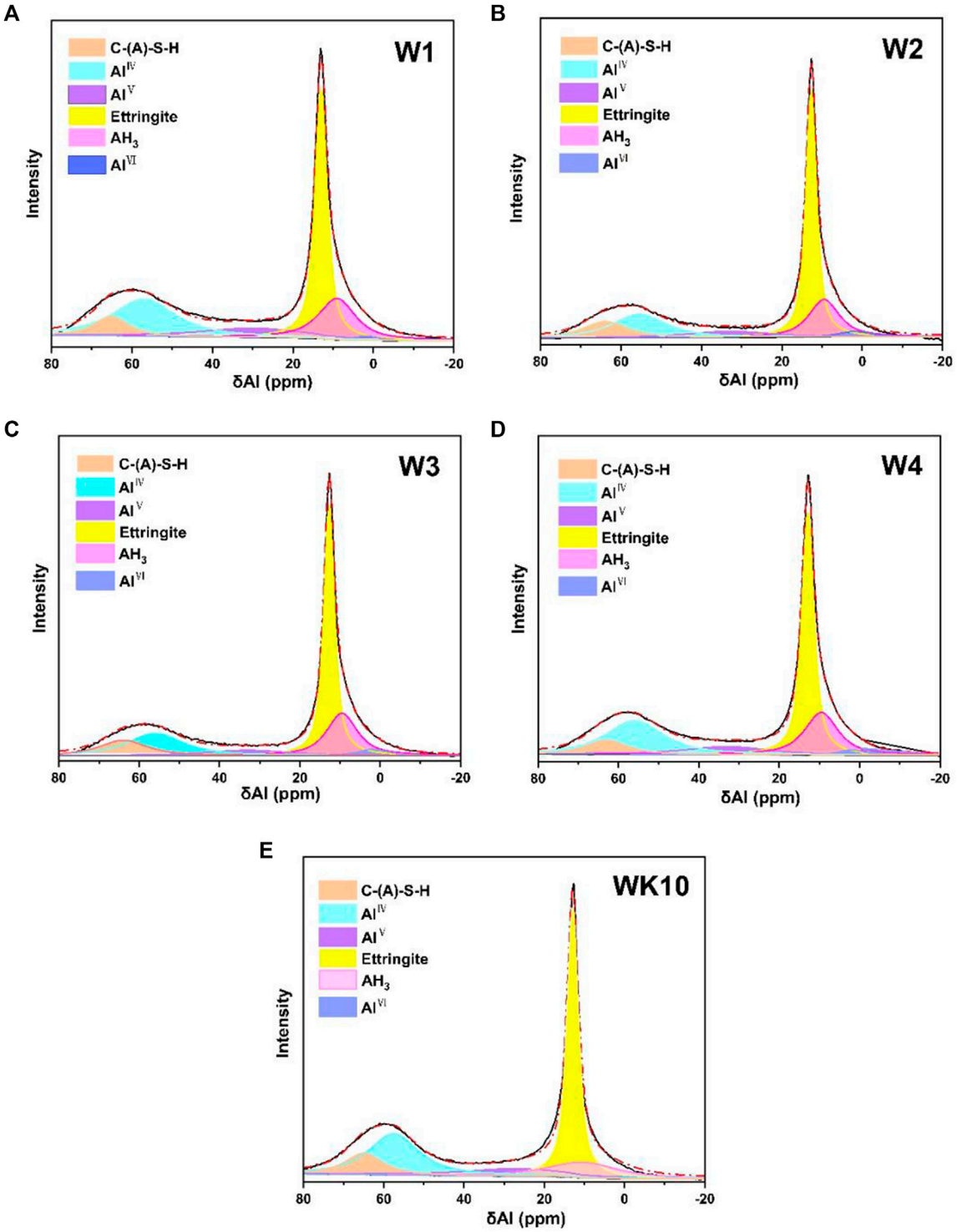

FIGURE 9 | ^{27}Al NMR deconvolution of P-SSC binders at 28 days: **(A)** W1, **(B)** W2, **(C)** W3, **(D)** W4, and **(E)** WK10.

ettringite or gels. In addition, the film formed by ettringite and C-A-S-H gel will parcel the slag particle and impede the hydration process further, decreasing the improvement rate of later strength. The sample incorporated metakaolin contains a high relative ratio of unreacted AlO, while the absolute content of AlO in ettringite and C-A-S-H gel is larger than that in other samples. It implies that wet-grinding P-SSC has a slight effect on the generation of ettringite and C-A-S-H gel because of the

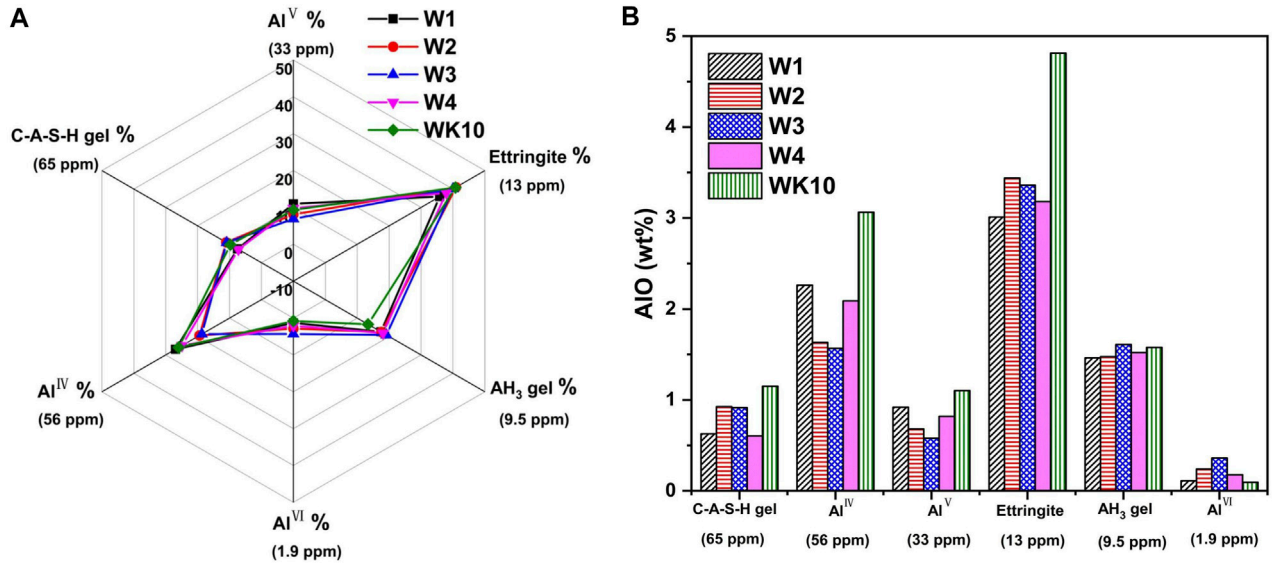

FIGURE 10 | (A) Relative and **(B)** absolute content associated with AlO signals in ^{27}Al NMR spectra.

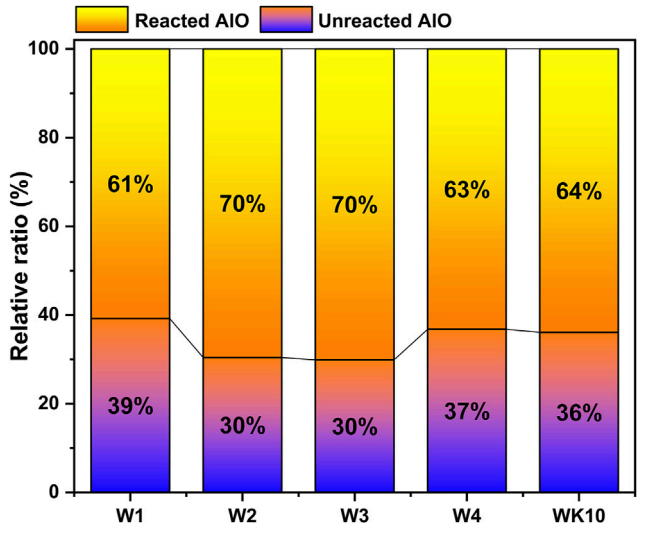

FIGURE 11 | Relative ratio of unreacted and reacted AlO in P-SSC binders at 28 d

relatively low content of the aluminum phase and dissolution rate compared to metakaolin. Increasing AlO_2^- concentration during this process by incorporating metakaolin can accelerate the hydration rate, resulting in more excellent strength development. However, the unreacted AlO and the generated AH_3 gel also indicate that the ettringite cannot form continuously by adding an amount of metakaolin in this cementitious system with low alkalinity.

As discussed before, the binding energy of main elements for slag before and after wet grinding is characterized by XPS to evaluate the activation of this preparation method for supplementary cementitious materials (**Figure 12**), among which oxygen, aluminum, silicon, and calcium are the critical components for the hydration phase. The high-resolution scan curves present a tendency to transfer to the left after wet grinding, implying the lower binding energies to a certain extent. For slag, the destruction of the surface structure by wet grinding weakens the bonding of atoms to electrons, where the chemical bonds are more likely to break for further hydration or polymerization, displaying higher instability and activeness. Published articles have demonstrated that activating coal gangue and fly ash by wet grinding attributes to the decrease in binding energy for Si 2p and Al 2p, which is consistent with the results of this study [39]. Combined with FTIR analysis, the wet grinding process is beneficial to improve the hydration activity of slag by destroying the surface structure. However, the enhancement effect is limited as the restricted time for wet grinding.

The mass loss of P-SSC binders at different temperature ranges is tested to discuss the content of each substance further. **Figure 13** describes that all P-SSC samples present two obvious peaks referred to as the DTG curves, which are related to the rapid decomposition of hydration products and gypsum. According to the previous research, the temperature range (20–800°C) can be divided into four periods based on the TG and DTG curves to distinguish the content of water in different substances, where the divided temperature ranges display a few differences due to the different microstructure of P-SSC. The initial period (20–80°C) and period II (140–180°C) are mainly associated with the loss of free water and crystal water in gypsum, respectively. Period I (80–140°C) depends on the decomposition of C-A-(S)-H gel and ettringite, and period III (180–800°C) is affected by the decomposition of AH_3 gel and continuous mass loss of C-(A)-S-H gels and ettringite [1, 40, 41]. For the samples with the same mix proportions, W2 and W3 present considerable mass loss during period I, meaning a high hydration degree. The mass loss in period III is the highest in W3 and WK10. On the one hand, it can reflect the AH_3 gel content, consistent with the FTIR and ^{27}Al NMR results. On

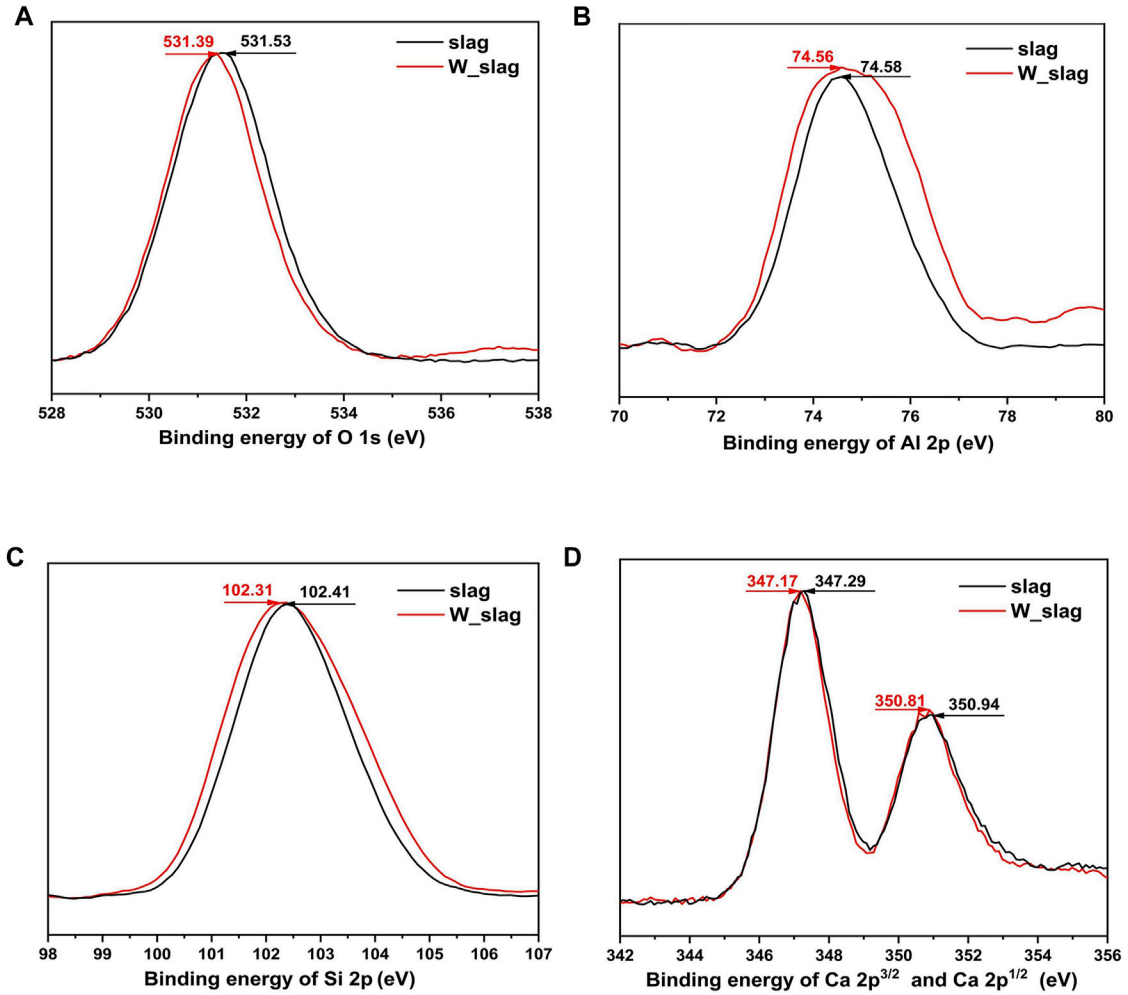

FIGURE 12 | (A) O 1s, **(B)** Al 2p, **(C)** Si 2p, **(D)** Ca $2p^{3/2}$, and Ca $2p^{1/2}$ high-resolution spectra of slag before and after wet milling.

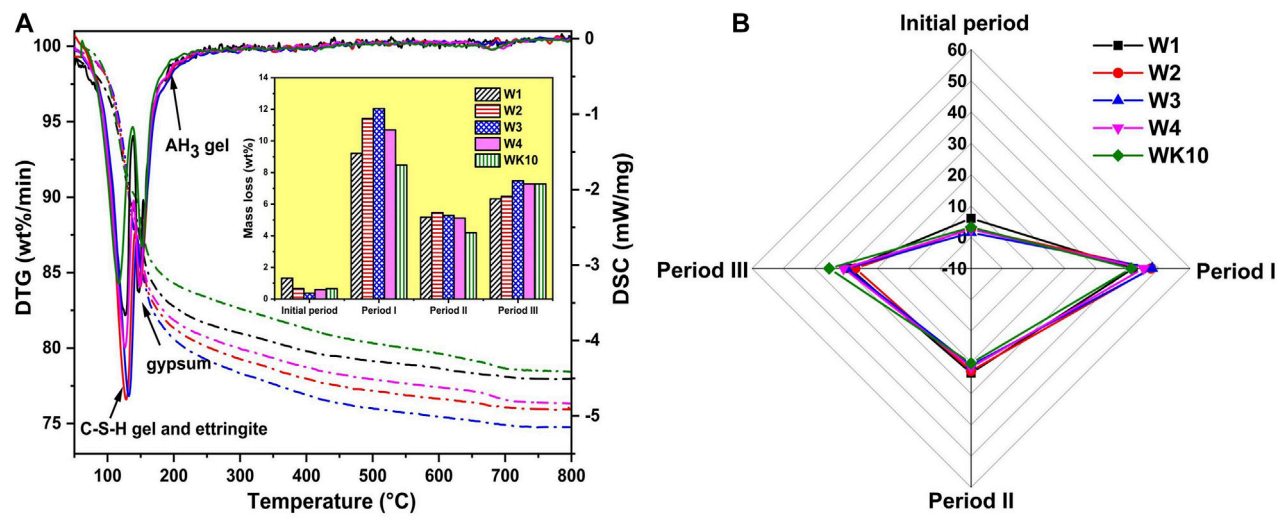

FIGURE 13 | (A) TG curves and **(B)** relative mass loss in each period for P-SSC binders at 28 days.

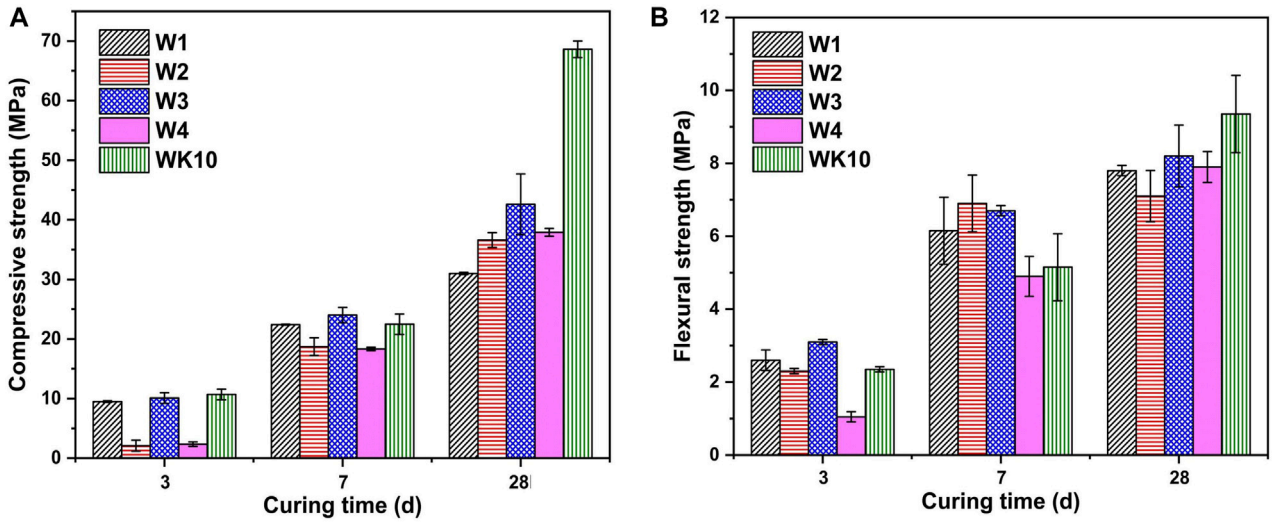

FIGURE 14 | (A) Compressive and **(B)** flexural strength development of P-SSC binders.

the other hand, the crystallinity of hydration products will affect the mass loss during this period: When the pore solution contains a high concentration of aluminate, portlandite, and gypsum, ettringite formed and precipitated rapidly will display a low crystallinity decomposition temperature, whereas ettringite with higher crystallinity will gradually lose structural water at higher temperatures.

The measured results of strength development for P-SSC binders shown in **Figure 14** indicate that the impurity release as the main factor determine the setting time and early strength development of the matrix. The lower early strength of W2 and W4 proves that the refinement and dispersion of wet grinding on raw materials can accelerate the formation of early hydration products such as ettringite, while it cannot compensate for the retard effect caused by the impurity release. Compared with W1, the optimization of early strength for W3 is slight as the limited refining of wet grinding on slag. It is observed that the strength development of W1 mainly occurs during the early hydration period (i.e., 3 days to 7 days), and the other samples show significant strength enhancement during the age of 7 days to 28 days. W3 has the optimal strength at each period, and its compressive strength and flexural strength reach 42.6 and 8.2 MPa, respectively, at 28 days. In addition, the refinement of phosphogypsum accelerates the formation of ettringite, while the dissolution of impurities has a negative influence on the later strength enhancement. The 28-day compressive strength of W2 and W4 only reaches 36.6 MPa and 37.9 MPa, respectively, and the flexural strength of W2 even displays a reduction. In comparison with other samples, the incorporation of metakaolin presents significant improvement during the wet grinding process, where the compressive and flexural strength of WK10 at 28 days reach 68.63 MPs and 9.35 MPa, respectively. However, WK10 presents comparable early strength with W3, and the increased ratio of later compressive strength reaches 205.34%. During the early hydration period, the impurity release caused by wet grinding plays a dominant role, which leads to the delay of early strength development. However, incorporating metakaolin with small particles optimizes the grain size distribution and provides extra aluminate for the rapid formation of ettringite, enhancing the later strength development.

The quantity of Ca^{2+}, SO_4^{2-}, OH^-, and AlO_2^- in pore solution determines the production of ettringite, as stated in **Eq. 5**. Published data have reported that increasing the concentration of Ca^{2+} is regarded as a practical approach for boosting the synthesis and stability of ettringite, referring to the solubility product constant (K_{sp}). The impurity precipitation in the pore solution after wet grinding, which will consume portlandite and delay the further hydration of cement, is also proved to impact the ettringite production. As the rapid dissolution rate of gypsum in the early hydration stage, Ca^{2+} and SO_4^{2-} in pore solution present relatively sufficient and significantly higher concentrations than AlO_2^-, as **Figure 15** described. Therefore, the dissolution and release rate of AlO_2^- are critical for the formation of ettringite. Combined with the existing experimental results, wet grinding has an excellent effect on the particles with larger dispersed sizes and improves the uniformity and stability of the new slurry, speeding up the hydration rate of phosphogypsum particles and promoting the generation of ettringite in the W2. While the quick precipitation of impurities displays a negative impact on the strength development. The destruction of the surface structure for slag by wet grinding accelerates the dissolution of active aluminosilicate groups, encouraging the formation of ettringite and C-(A)-S-H gel. Therefore, W3 shows the optimal mechanical properties, where ettringite shows a significant improvement for compressive strength, while the generation of C-A-S-H gel seems to have a more comparable enhancement on the flexural strength. However, due to the relatively small particle size and low aluminum content for slag, the improvement of the hydration degree during the wet grinding process is limited, presenting a slight increase in the AlO_2^- concentration in the pore solution.

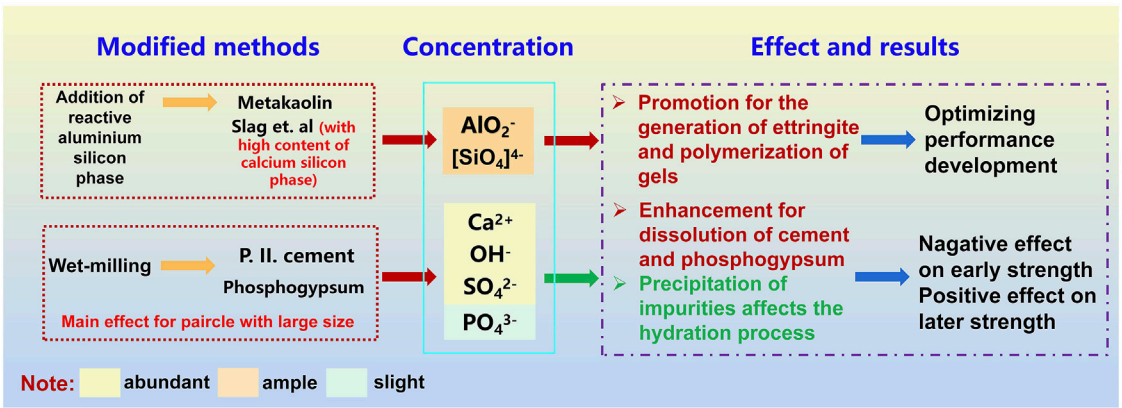

FIGURE 15 | Effect of wet grinding and incorporated aluminum phases on the hydration of P-SSC binders.

Therefore, compared with the sample containing metakaolin, lower strength development is noticed in all groups with limited performance optimization at each period. However, the existence of unreacted AlO and AH_3 gel illustrates that the addition of metakaolin with a low calcium content has a critical value. In the absence of portlandite in this system, the excess will impact the continuous hydration of P-SSC binders, leading to a lower hydration degree.

$$K_{sp} = \frac{[3CaO \cdot Al_2O_3 \cdot 3CaSO_4 \cdot 32H_2O]}{[Ca^{2+}]^6 \cdot [SO_4^{2-}]^3 \cdot [OH^-]^4 \cdot [AlO_2^-]^2 \cdot [H_2O]^{29}} \quad (5)$$

CONCLUSION

In this study, the mechanism of wet grinding on the hydration process of particles in the P-SSC pastes was investigated, and the improvement of the active aluminum phase on the hydration product generation was discussed further by incorporating metakaolin. Based on the experimental results, it is possible to draw the following conclusions:

(1) Wet grinding presents a significant improvement in the refining and dispersion of particles of large sizes, while limited optimization is observed for small-size particles. Wet grinding increases the dissolution rate and supersaturation of phosphogypsum, the destruction of surface structure for slag also enhances the hydration rate and degree of P-SSC pastes by releasing more silicon (aluminum) oxygen tetrahedron groups. More extensive content of gels with higher polymerization and ettringite is noticed in the P-SSC matrix.
(2) Rapid dissolution of phosphogypsum is accompanied by the release of impurities. The refining effect of wet grinding on the phosphogypsum structure promotes the further release of impurities which harms strength development. Although strength enhancement of P-SSC pastes after wet grinding becomes conspicuous at the later hydration stage, the amount of generated ettringite shows a slight increase as the small content of the aluminum phase in the slag, leading to the limited optimization of mechanical properties.
(3) The incorporation of metakaolin with a high content of active aluminum phases has a remarkable enhancement on the hydration degree of P-SSC pastes during the wet grinding process. In the sulfate-rich environment, adding metakaolin accelerates the release rate of AlO_2^-, which is regarded as a vital factor for the generation of ettringite. For P-SSC pastes, ettringite crystallized from the unsaturated portlandite solution presents negligible crystallization pressure, which existed in pores, and creak is beneficial for the promotion of density and strength.
(4) Therefore, preparing P-SSC pastes by wet grinding and incorporating supplement cementitious materials containing a high content of active aluminum phase can effectively optimize the performance of this eco-friendly cementitious material, realizing the large-scale application of phosphogypsum in the building materials industry.

DATA AVAILABILITY STATEMENT

The original contributions presented in the study are included in the article/Supplementary Material, further inquiries can be directed to the corresponding author.

AUTHOR CONTRIBUTIONS

ZW: conceptualization, formal analysis, writing—original draft, and software. ZS: funding acquisition and project administration. TS: methodology, supervision, and writing—review and editing. ZL: validation.

ACKNOWLEDGMENTS

The authors gratefully acknowledge the financial support from the Key Research and Development Program of Hubei Province

(2020BAB065) Fundamental Research Funds for the Central Universities (No. 205259003); the Third Batch of Special Fund for Science and Technology Development of Zhongshan city in 2020 (2020-18), Sanya Yazhou Bay Science and Technology City Administration (No. SKJC-KJ-2019KY02), and Research Project of Advanced Engineering Technology Research Institute of the Wuhan University of Technology in Zhongshan City (WUT202011).

REFERENCES

1. Gijbels K, Nguyen H, Kinnunen P, Schroeyers W, Pontikes Y, Schreurs S, et al. Feasibility of Incorporating Phosphogypsum in Ettringite-Based Binder from Ladle Slag. *J Clean Prod* (2019) 237:117793. doi:10.1016/j.jclepro.2019.117793
2. Huang Y, Lin Z, Shui Z. *Excess-Sulfate Phosphogypsum Slag Cement and Concrete*. Wuhan: Wuhan University of Technology Press (2010).
3. Huang Y, Lin Z. Investigation on Phosphogypsum-Steel Slag-Granulated Blast-Furnace Slag-limestone Cement. *Construction Building Mater* (2010) 24(7):1296–301. doi:10.1016/j.conbuildmat.2009.12.006
4. Ding S. *Research on Corrosion Resistance and its Mechanism of Persulfur Phosphogypsum-Slag Cement concrete under Sea Salt Environment*. Wuhan: Wuhan university of technology, Wuhan university of technology (2014).
5. Lu J. *Research on the Preparation and Durability of Persulfur Phosphogypum Slag Cement concrete*. Wuhan: Material, Wuhan University of Technology (2013).
6. Peng J, Wan T. Effect of Impurity Composition, Morphology and Distribution on Properties of Phosphogypsum. *Chin Build Mater.Technol* (0062) 000:31–5.
7. Park H, Jeong Y, Jun Y, Jeong J-H, Oh JE. Strength Enhancement and Pore-Size Refinement in Clinker-free CaO-Activated GGBFS Systems through Substitution with gypsum. *Cement and Concrete Composites* (2016) 68: 57–65. doi:10.1016/j.cemconcomp.2016.02.008
8. Wang L, Liu S. Research Review on Ettringite Phase. *Concrete* (2013) 8: 83–90.
9. Shi Y, Wang Z, Wu D, Zhang H. Formation Conditions and Stability of Ettringite. *Concrete* (2000) 8:52–4.
10. Wang S, Ji S, Liu Y, Hu K. Influence of Alkali on Expansion Property of Sulphoaluminate Cement. *J Chin Ceram Soc* (1986) 14(3):285–93.
11. Lou Z, Xu X, Han R, Liu C. On the Formation and Reaction of Ettringite in Slag Cement. *J Chin Ceram Soc* (1981) 9(3):295–301.
12. Peng J, Lou Z. Study on the Mechanism of Ettringite. *J Chin Ceram Soc* (2000) 28(6):511–5.
13. Damidot D, Glasser FP. Thermodynamic Investigation of the CaO-Al_2O_3-$CaSO_4$-H_2o System at 25°C and the Influence of Na_2O. *Cement Concrete Res* (1993).
14. Siddique R, Khan MI. *Supplementary Cementing Materials*. Supplementary Cementing Materials2011.
15. Yang J, Huang J, Su Y, He X, Tan H, Yang W, et al. Eco-friendly Treatment of Low-Calcium Coal Fly Ash for High Pozzolanic Reactivity: A Step towards Waste Utilization in Sustainable Building Material. *J Clean Prod* (2019) 238: 117962. doi:10.1016/j.jclepro.2019.117962
16. Liu S, Wang L, Yu B. Effect of Modified Phosphogypsum on the Hydration Properties of the Phosphogypsum-Based Supersulfated Cement. *Construction Building Mater* (2019) 214:9–16. doi:10.1016/j.conbuildmat.2019.04.052
17. Kotake N, Kuboki M, Kiya S, Kanda Y. Influence of Dry and Wet Grinding Conditions on Fineness and Shape of Particle Size Distribution of Product in a ball Mill. *Adv Powder Tech* (2011) 22(1):86–92. doi:10.1016/j.apt.2010.03.015
18. Kristaly F, Kumar S, Mucsi G, Pekker P. Mechanical Activation of Fly Ash and its Influence on Micro and Nano-Structural Behaviour of Resulting Geopolymers. *Adv Powder Technol internation J Soc Powder Technol Jpn* (2017) 28(3):805–13.
19. Tan H, Nie K, He X, Deng X, Zhang X, Su Y, et al. Compressive Strength and Hydration of High-Volume Wet-Grinded Coal Fly Ash Cementitious Materials. *Construction Building Mater* (2019) 206:248–60. doi:10.1016/j.conbuildmat.2019.02.038
20. He X, Ye Q, Yang J, Dai F, Su Y, Wang Y, et al. Physico-chemical Characteristics of Wet-Milled Ultrafine-Granulated Phosphorus Slag as a Supplementary Cementitious Material. *J Wuhan Univ Technol.-Mat Sci Edit* (2018) 33(3):625–33. doi:10.1007/s11595-018-1870-4
21. Strandard CN. *GB/T 1346-2011: Test Methods for Water Requirement of normal Consistency, Setting Time and Soundness of the portland Cement*. Beijing: N.C.S. Committee (2012).
22. Han J, Shui Z, Wang G, Sun T, Gao X. Performance Evaluation of Steam Cured HPC Pipe Piles Produced with Metakaolin Based mineral Additives. *Construction Building Mater* (2018) 189:719–27. doi:10.1016/j.conbuildmat.2018.09.044
23. Xia X, Zhang X, Cao C. Magnetic alloy Micrograph Indication Based on Semi-quantitative Component Analysis by RIR Method. *J Jinggangshan Univ (Nat Sci* (2010) 31(5):35–7.
24. Fang D, He F, Xie J, Lihui X. Calibration of Binding Energy Positions with C1s for XPS Results. *J Wuhan Univ Technology(Materials Science)* (2020)(4). doi:10.1007/s11595-020-2312-7
25. CN. *Standard, GB/T1767-1999: Method of Testing Cements-Determination of Strength*. Beijing: N.C.S. Committee (1999).
26. Nakach M, Authelin J-R, Chamayou A, Dodds J. Comparison of Various Milling Technologies for Grinding Pharmaceutical Powders. *Int J Mineral Process* (2004) 74(Suppl. S):S173–S181. doi:10.1016/j.minpro.2004.07.039
27. Matijai G, Kurajica S. Grinding Kinetics of Amorphous Powder Obtained by Sol–Gel Process. *Powder Technol* (2010) 197(3):165–9.
28. Choi WS, Yoon BR. Applications of Grinding Kinetics Analysis to fine Grinding Characteristics of Some Inorganic Materials Using a Composite Grinding media by Planetary ball Mill. *Powder Technol* (2001) 115(3):209–14.
29. Derjaguin B, Landau L. Theory of the Stability of Strongly Charged Lyophobic Sols and of the Adhesion of Strongly Charged Particles in Solutions of Electrolytes. *Prog Surf Sci* (1993) 43(1-4):30–59. doi:10.1016/0079-6816(93)90013-l
30. Verwey EJW, Overbeek JTG. Theory of the Stability of Lyophobic Colloids. *J Colloid Sci* (1955) 10(2):224–5. doi:10.1016/0095-8522(55)90030-1
31. Gsa B, Jz B, Na YB. Microstructural Evolution and Characterization of Ground Granulated Blast Furnace Slag in Variant pH. *Constr Build Mater* 251.
32. Scholtzová E, Kucková L, Kožíšek J, Tunega D. Structural and Spectroscopic Characterization of Ettringite mineral–combined DFT and Experimental Study. *J Mol Struct* (2015) 1100:215–24.
33. Higl J, Hinder D, Rathgeber C, Ramming B, Lindén M. Detailed *In Situ* ATR-FTIR Spectroscopy Study of the Early Stages of C-S-H Formation during Hydration of Monoclinic C3S. *Cement Concrete Res* (2021) 142:106367. doi:10.1016/j.cemconres.2021.106367
34. Sba B, Mt C, Clb C, D The B. Effect of Equilibration Time on Al Uptake in C-S-H. *Cement Concrete Res* 144.
35. Boumaza A, Mekhalif Z, Djebaili K, Djelloul XPS. FTIR, EDX, and XRD Analysis of Al_2O_3 Scales Grown on PM2000 Alloy. *J Spectrosc* (2015).
36. Liu C, Shih K, Gao Y, Li F, Lan W. Dechlorinating Transformation of Propachlor through Nucleophilic Substitution by Dithionite on the Surface of Alumina. *J Soils Sediments* (2012) 12(5). doi:10.1007/s11368-012-0506-0
37. Padilla-Encinas P, Palomo A, Blanco-Varela MT, Fernández-Jiménez A. Calcium Sulfoaluminate Clinker Hydration at Different Alkali Concentrations. *Cement Concrete Res* (2020) 138:106251. doi:10.1016/j.cemconres.2020.106251
38. Deng G, He Y, Lu L, Hu S. The Effect of Activators on the Dissolution Characteristics and Occurrence State of Aluminum of Alkali-Activated Metakaolin. *Construction Building Mater* (2020) 235:117451. doi:10.1016/j.conbuildmat.2019.117451

39. Li C, Wan J, Sun H, Li L. Investigation on the Activation of Coal Gangue by a New Compound Method. *J Hazard Mater* (2010) 179(1-3):515–20. doi:10.1016/j.jhazmat.2010.03.033
40. Wang S-D, Scrivener KL. Hydration Products of Alkali Activated Slag Cement. *Cement Concrete Res* (1995) 25(3):561–71. doi:10.1016/0008-8846(95)00045-e
41. Chang H, Jane Huang P, Hou SC. Application of Thermo-Raman Spectroscopy to Study Dehydration of CaSO4·2H2O and CaSO4·0.5H2O. *Mater Chem Phys* (1999) 58(1):12–9. doi:10.1016/s0254-0584(98)00239-9

Conflict of Interest: The authors declare that the research was conducted in the absence of any commercial or financial relationships that could be construed as a potential conflict of interest.

Publisher's Note: All claims expressed in this article are solely those of the authors and do not necessarily represent those of their affiliated organizations, or those of the publisher, the editors, and the reviewers. Any product that may be evaluated in this article, or claim that may be made by its manufacturer, is not guaranteed or endorsed by the publisher.